Title

Selective oxidation and oxidative dehydrogenation of hydrocarbons on bismuth vanadium molybdenum oxide

Authors

Zhai, Zheng
Wang, Xuan
Licht, Rachel
et al.

Publication Date

2015-05-01

DOI

10.1016/j.jcat.2015.02.015

Peer reviewed

Journal of Catalysis 325 (2015) 87–100

Contents lists available at ScienceDirect

Journal of Catalysis

journal homepage: www.elsevier.com/locate/jcat

Selective oxidation and oxidative dehydrogenation of hydrocarbons on bismuth vanadium molybdenum oxide

Zheng Zhai, Xuan Wang, Rachel Licht, Alexis T. Bell *

Department of Chemical and Biomolecular Engineering, The University of California Berkeley, Berkeley, CA 94720-1462, USA

ARTICLE INFO

Article history:
Received 6 January 2015
Revised 16 February 2015
Accepted 22 February 2015
Available online 19 March 2015

Keywords:
Bismuth vanadium molybdenum oxide
Selective oxidation
Oxidative dehydrogenation
Butene

ABSTRACT

A systematic investigation of the oxidative dehydrogenation of propane to propene and 1- and 2-butene to 1,3-butadiene, and the selective oxidation of isobutene to methacrolein was carried out over $Bi_{1-x/3}V_{1-x}Mo_xO_4$ ($x = 0–1$) with the aim of defining the effects of catalyst and reactant composition on the reaction kinetics. This work has revealed that the reaction kinetics can differ significantly depending on the state of catalyst oxidation, which in turn depends on the catalyst composition and the reaction conditions. Under conditions where the catalyst is fully oxidized, the kinetics for the oxidation of propene to acrolein and isobutene to methacrolein, and the oxidative dehydrogenation of propane to propene, 1-butene and trans-2-butene to butadiene are very similar—first order in the partial pressure of the alkane or alkene and zero order in the partial pressure of oxygen. These observations, together with XANES and UV–Vis data, suggest that all these reactions proceed via a Mars van Krevelen mechanism involving oxygen atoms in the catalysts and that the rate-limiting step involves cleavage of the weakest C—H bond in the reactant. Consistent with these findings, the apparent activation energy and pre-exponential factor for both oxidative dehydrogenation and selective oxidation correlate with the dissociation energy of the weakest C—H bond in the reactant. As the reaction temperature is lowered, catalyst reoxidation can become rate-limiting, the transition to this regime depending on ease of catalyst reduction and effectiveness of the reacting hydrocarbons as a reducing agent. A third regime is observed for isobutene oxidation at lower temperatures, in which the catalyst is more severely reduced and oxidation now proceeds via reaction of molecular oxygen, rather than catalyst lattice oxygen, with the reactant.

1. Introduction

The oxidation of propene to acrolein and isobutene to methacrolein and the oxidative dehydrogenation of *n*-butene to 1,3-butadiene are used to produce commodity chemicals and monomers for a variety of polymers. Most of the catalysts used to promote these reactions are based on bismuth molybdate to which other metals are added to enhance activity and product selectivity [1–22]. For this reason, there is considerable interest in understanding the influence of catalyst composition on catalyst activity and selectivity reaction process, and the effects of reactant composition on rate of product formation and the distribution of products formed. Surprisingly, though, there have been relatively few in depth investigations conducted on this subject.

Of the several systems of interest, the one that has been investigated most extensively is the oxidation of propene to acrolein over bismuth molybdate. This reaction has been shown to proceed via a Mars van Krevelen mechanism [23]. The rate-limiting step has been shown to involve the abstraction of an H atom from the methyl group of propene to form an allyl intermediate, which is then stabilized on the catalyst surface as a vinyl alkoxide. Acrolein is then produced by the abstraction of a second H atom from the alkoxide species [24,25]. Much less is known, though, about the reactions of other hydrocarbons over bismuth molybdate-based catalysts. Studies of the oxidative dehydrogenation of *n*-butenes to butadiene over bismuth molybdate have been carried out, and mechanism for this reaction is thought to resemble that for the oxidation of propene [26–30]. On the other hand, several different mechanisms have been proposed for the oxidation of isobutene to methacrolein, including a Langmuir–Hinshelwood mechanism and a redox model [31–33].

It is notable that previous studies of reaction mechanism and kinetics have tended to be reactant specific, and very few have involved a systematic investigation of the effects of catalyst and reactant composition. A notable exception has been the case of propene oxidation to acrolein over $Bi_{1-x/3}V_{1-x}Mo_xO_4$ ($x = 0–1$) [34] prepared with a scheelite structure. Ueda et al. [12] and Sleight et al. [35,36] have reported that $Bi_{1-x/3}V_{1-x}Mo_xO_4$ is more active for the oxidation of propene than either bismuth molybdate

* Corresponding author.
E-mail address: bell@cchem.berkeley.edu (A.T. Bell).

http://dx.doi.org/10.1016/j.jcat.2015.02.015
0021-9517/

($x = 1$) or bismuth vanadate ($x = 0$). Our previous work proposed a generalized model for the kinetics of propene oxidation over $Bi_{1-x/3}V_{1-x}Mo_xO_4$, and explained the exact roles of Bi, Mo, and V in affecting the activity and selectivity of $Bi_{1-x/3}V_{1-x}Mo_xO_4$ [37–39]. By contrast, very little is known about the oxidation and oxidative dehydrogenation of butene isomers over vanadium-substituted bismuth molybdate. Therefore, many questions are still open. For example, will both reactions follow a mechanism similar to that propene oxidation for all catalyst compositions, and how does the composition and structure of the reactant affect reactant reactivity? Another question not fully understood is whether the reaction kinetics are the same independent of reaction conditions and if different for different reaction conditions, what are the mechanistic implications?

The work reported here was undertaken in order to determine catalyst and reactant composition, as well as reaction conditions affect the kinetics for the oxidative dehydrogenation of propane and 1- and 2-butene, and the selective oxidation of propene and isobutene over $Bi_{1-x/3}V_{1-x}Mo_xO_4$. The oxidation state of the catalyst reduction was probed by in situ XANES and UV–Vis spectroscopy. The results of this work demonstrate that $Bi_{1-x/3}V_{1-x}Mo_xO_4$ can operate in one of three regimes depending on the reactant and catalyst composition, the reaction temperature, and the partial pressure of the reactants. Under conditions where the catalyst is maintained in its fully oxidized state, all reactions follow a Mars van Krevelen mechanism. Under these conditions, the reaction kinetics are first order in the partial pressure of the reactant and zero order in oxygen, and both the apparent activation energy and the apparent pre-exponential factor increase with the strength of the weakest C—H bond of the reactant involved in the rate-limiting step. When the rate of catalyst reoxidation cannot keep up with the rate of catalyst reduction, the reaction becomes zero order in reactant and fractional order in oxygen partial pressure. In this case, the apparent activation energy and pre-exponential factor become independent of the reactant composition and reflective of the activation energy for catalyst reoxidation. When the catalyst is more severely reduced, reaction kinetics become inverse order in reactant and first order in oxygen partial pressure. Under these conditions, the apparent activation energy is very high and the reaction is thought to proceed via the reaction of adsorbed molecular O_2 and the reactant.

2. Methods

2.1. Catalyst preparation

Catalysts were prepared by the complexation procedure [37]. The metal precursors, ammonium molybdate tetrahydrate (99.98%, Sigma–Aldrich), bismuth (III) nitrate pentahydrate (99.98%, Sigma–Aldrich), and ammonium metavanadate (99%, Sigma–Aldrich), at the atomic ratios of Bi:V:Mo = $(1 - x/3):(1 - x):x$ ($x = 0$–1.0), were mixed with citric acid (1:1 M ratio with metal precursors) to produce materials with the stoichiometry $Bi_{1-x/3}V_{1-x}Mo_xO_4$. Metal precursors with citric acid were dissolved separately and then mixed together slowly. 2 M HNO_3 was used in place of water to dissolve bismuth nitrate to prevent precipitation of bismuth hydroxides. The resulting solution was dried at 60 °C for about 24 h in air to form a gel, which was then dried at 120 °C and calcined in flowing air at 600 °C for 6 h. Powdered catalysts were obtained.

2.2. Catalyst characterization

X-ray absorption spectroscopy (XAS) measurements were performed at the Advanced Photon Source at Argonne National Laboratory (ANL) on beam line 10BM. Measurements were performed as described previously [37]. Data were acquired at the Bi L_3-edge, and at the Mo and V K-edges before and after exposure to reactant at 713 K. Additional data were acquired in situ at the Mo K-edge under steady-state reaction conditions. These experiments were carried out in a controlled-atmosphere cell that could be heated up to 743 K in the presence of flowing gas [40].

Diffuse reflectance UV–VIS-NIR spectra were acquired using a Fischer Scientific EVO 300 spectrometer equipped with a Praying Mantis reflectance chamber and an in-situ high-pressure cell (Harrick Scientific, Inc.). Spectra were referenced to the diffuse reflectance spectrum of a Teflon reference.

2.3. Catalyst activity and selectivity

Measurements of reaction rates and product distributions were performed using a packed-bed quartz tube reactor (10 mm in diameter) loaded with 50–200 mg of catalyst. Prior to reaction, the catalyst was preheated to the reaction temperature in air. All experiments were carried out at atmospheric pressure with 3.3–16.7% propene (99.9%, Praxair), 1-butene (99%, Praxair), trans-2-butene (99%, Praxair), isobutene (99%, Praxair), propane (99%, Praxair), and 3.3–16.7% oxygen (supplied from 20% oxygen in helium, Praxair), balanced as needed with additional helium (99.995%, Praxair). Data were collected at steady state between 573 K and 713 K. Products were analyzed using a gas chromatograph (Agilent 6890A) equipped with a 30 m HP-PLOT Q column and a flame ionization detector (FID), for analyzing hydrocarbons. An Alltech Hayesep DB packed column connected to a thermal conductivity detector (TCD) was used to analyze for oxygen, and carbon mono- and di-oxides. Reactant conversion was calculated on the basis of products formed. Product selectivity was defined as the moles of reactant converted to the product over the sum of the moles of reactant converted to all products, based on a carbon balance. All selectivities reported in this study are intrinsic selectivities, extrapolated to a conversion of <1%.

3. Results

3.1. Kinetics

3.1.1. Product distribution

The main product of 1-butene and trans-2-butene oxidation over $Bi_{1-x/3}V_{1-x}Mo_xO_4$ is 1,3-butadiene, and the principle by-products are trans-, cis-2-butene, and 1-butene. The influence of vanadium content on catalyst activity for 1,3-butadiene formation from 1-butene and trans-2-butene is presented in Fig. 1. In both cases, the activity passes through a maximum at $x = 0.45$ in a manner similar to that observed for propene oxidation to acrolein production over the same catalysts [37].

The selectivities to products formed from 1-butene and trans-2-butene are presented in Fig. 2. For both 1-butene and trans-2-butene, the product selectivities are similar and in each case the main product is 1,3-butadiene. However, the selectivity to 1,3-butadiene is higher starting from 1-butene than from trans-2-butene. For both isomers of butene, the selectivity to 1,3-butadiene passes through a shallow minimum at $x = 0.45$ with increasing value of x. By contrast, the selectivity to isomers of the reactant passes through a maximum at the same value of x.

The main product of isobutene oxidation is methacrolein, and the principle by-products are CO, CO_2, and ethene. As shown in Fig. 3, the activity for methacrolein formation at 703 K increases with the value of x, and then reaches a maximum for $Bi_{0.85}Mo_{0.45}V_{0.55}O_4$ ($x = 0.45$). Product selectivities are also presented in Fig. 3. The selectivity to methacrolein is 55% for $x = 0$,

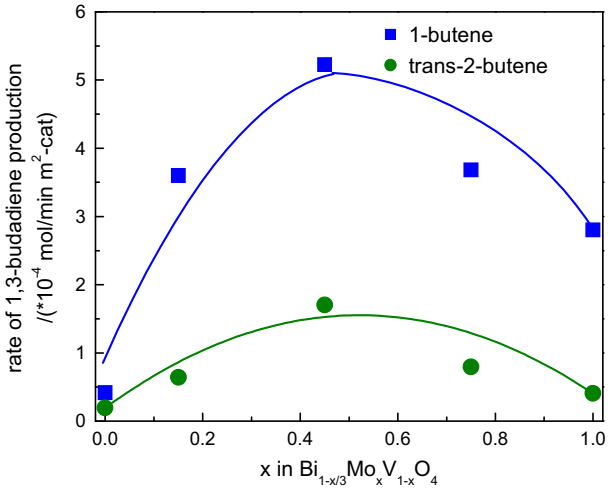

Fig. 1. Variation in the rate of the oxidative dehydrogenation of 1-butene and trans-2-butene to 1,3-butadiene on $Bi_{1-x/3}V_{1-x}Mo_xO_4$ with x at 673 K. Total flow rate: 60 mL/min. Left: 1-butene, P_{1-C4H8} = 0.067 atm, P_{O2} = 0.167 atm. Right: trans-2-butene, $P_{trans\text{-}2\text{-}C4H8}$ = 0.067 atm, P_{O2} = 0.167 atm.

rises slightly to 60% for x = 0.45, and then decreases to 48% for x = 1.0. CO_2 and CO (CO_x) are the primary by-products, and selectivity to CO_x follows a trend with catalyst composition that is opposite to that for methacrolein. The selectivity to methacrolein observed for isobutene oxidation is about 10% lower than that to acrolein for propene reported for identical reaction conditions and catalysts [37]. It is notable, though, that the rate of methacrolein formation at a lower temperature (673 K) and a higher partial pressure of isobutene (0.067 atm) is nearly independent of the value of x (Fig. 4). The product selectivities for $BiVO_4$ are identical than those observed at 703 K and a propene partial pressure of 0.0167 atm (Fig. 3). However, for Bi_2MoO_{12} and $Bi_{0.85}V_{0.55}Mo_{0.45}O_4$, the selectivity to methacrolein (40%) is about 10% lower and the selectivity to CO_2 is 10% higher than those observed at 703 K and a propene partial pressure of 0.167 atm.

Fig. 5 illustrates the effects of catalyst composition on the activity and product selectivities for the oxidative dehydrogenation of propane over $Bi_{1-x/3}V_{1-x}Mo_xO_4$. The main product in this case is propene, and the activity at 753 K is shown in Fig. 5. The main by-products are acrolein and CO_2. The product selectivities are also shown in Fig. 5. The selectivities to propene and CO_2 pass through shallow minima near x = 0.45, whereas the selectivity to acrolein passes through a weak maximum at the same value of x.

3.1.2. Partial pressure dependences

The rate of 1,3-butadiene formation from both 1-butene and trans-2-butene can be represented by

$$\text{rate}_{1,3\text{-butadiene}} = k_{app} P^m_{1,2\text{-}C_4H_8} P^n_{O_2} \quad (1)$$

where m and n are the apparent reaction orders of the partial pressure of butenes and oxygen. Values of m and n are given in Tables 1 and 2 at temperatures of 673 K and 693 K (the high temperature range) and 633 K (the low temperature range) for values of x = 0, 0.45, and 1.0.

For $BiVO_4$ and $Bi_2Mo_3O_{12}$, the data show that for both the high- and low-temperature regimes, the rate of 1-butene (and trans-2-butene) oxidation to 1,3-butadiene is nearly first order with respect to the partial pressure of the alkene and nearly zero order with respect to the partial pressures of O_2, regardless of the temperature. The observed reaction orders are identical to those reported by Keizer et al. [41] for the oxidative dehydrogenation of 1-butene over $Bi_2Mo_3O_{12}$ at temperatures between 541 K and 688 K.

For $Bi_{0.85}Mo_{0.45}V_{0.55}O_4$, the reaction orders were observed to vary with temperature for both reactants. The alkene partial pressure dependence increased from nearly zero order at low temperature (633 K) to close to first order at high temperature (673 and 693 K), whereas the oxygen partial pressure dependence decreased from a positive fractional order at lower temperatures to zero order at higher temperatures.

The rate of isobutene oxidation to methacrolein can be represented by

$$\text{rate}_{\text{methacrolein}} = k_{app} P^m_{\text{iso-}C_4H_8} P^n_{O_2} \quad (2)$$

Table 3 lists the apparent reaction orders for methacrolein production. At both 673 K and 703 K, the isobutene partial pressure dependence over $BiVO_4$ is close to unity and the oxygen partial pressure dependence is nearly zero order. For $Bi_2Mo_3O_{12}$ and $Bi_{0.85}Mo_{0.45}V_{0.55}O_4$, the reactant partial pressure dependences at 703 K are again first order in isobutene and zero order in oxygen. However, at 673 K, the dependence on isobutene partial pressure becomes negative first order and the oxygen partial pressure dependence becomes nearly first order for both $Bi_2Mo_3O_{12}$ and $Bi_{0.85}Mo_{0.45}V_{0.55}O_4$.

Table 4 shows the reaction orders for propane dehydrogenation to propene at 773 K. As expected, the rate of propene formation is first order in propane and zero order in oxygen for all values of x.

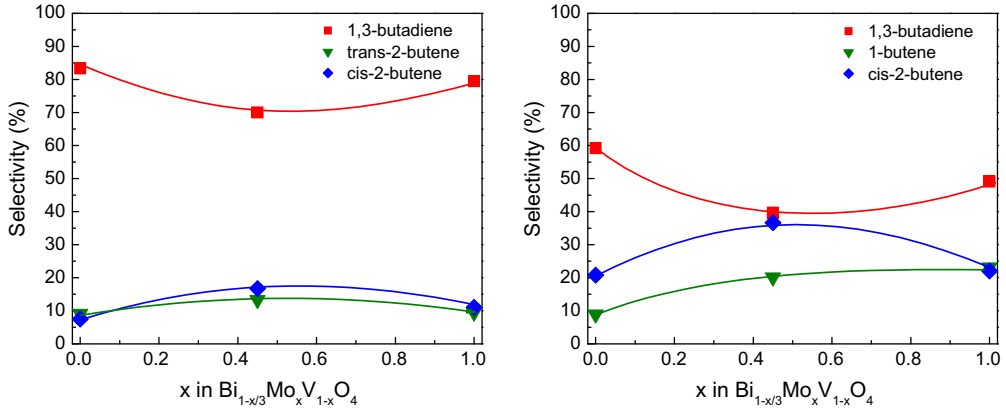

Fig. 2. Dependence of the selectivity of $Bi_{1-x/3}V_{1-x}Mo_xO_4$ for the oxidative dehydrogenation of 1-butene and trans-2-butene at 673 K. Left: 1-butene, $P_{1\text{-}C4H8}$ = 0.067 atm, P_{O2} = 0.167 atm. Right: trans-2-butene, $P_{trans\text{-}2\text{-}C4H8}$ = 0.067 atm, P_{O2} = 0.167 atm.

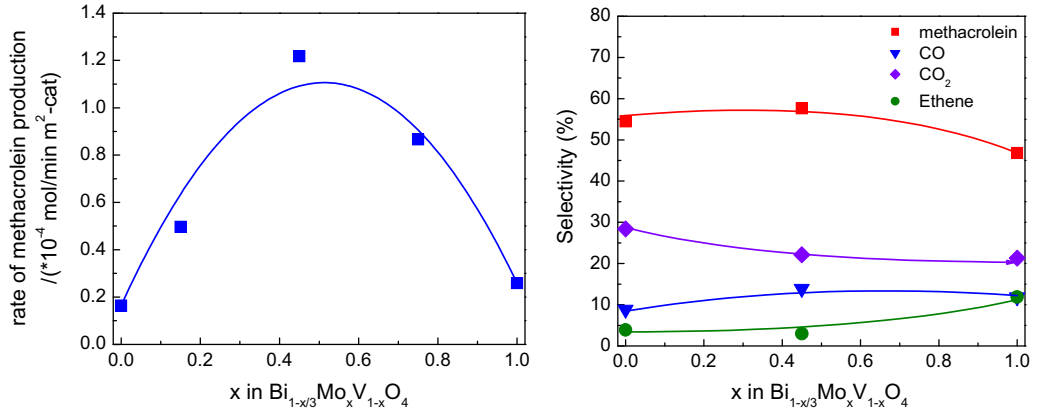

Fig. 3. Variation in the rate and selectivity of iso-butene oxidation to methacrolein on $Bi_{1-x/3}V_{1-x}Mo_xO_4$ with *x*. For rate measurement total flow rate: 60 mL/min. $P_{iso\text{-}C4H8}$ = 0.0167 atm, P_{O2} = 0.167 atm, 703 K.

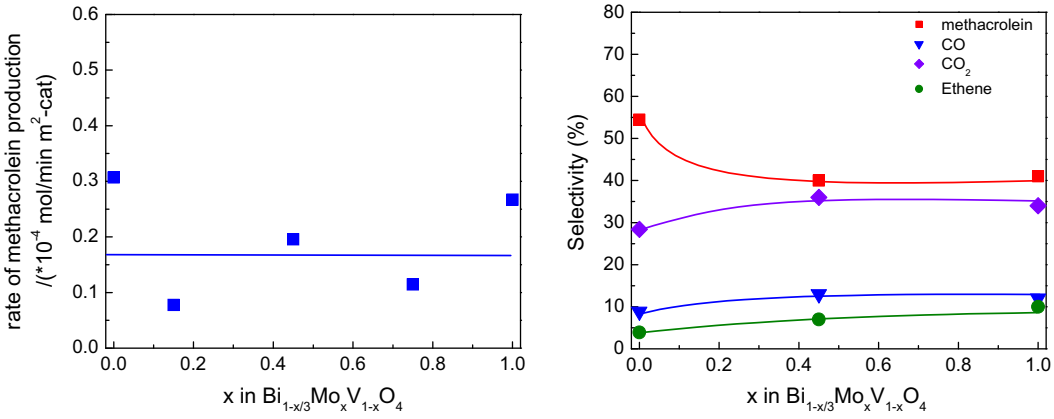

Fig. 4. Variation in the rate and selectivity of iso-butene oxidation to methacrolein on $Bi_{1-x/3}V_{1-x}Mo_xO_4$ with *x*. For rate measurement total flow rate: 60 mL/min. $P_{iso\text{-}C4H8}$ = 0.067 atm, P_{O2} = 0.167 atm, 673 K.

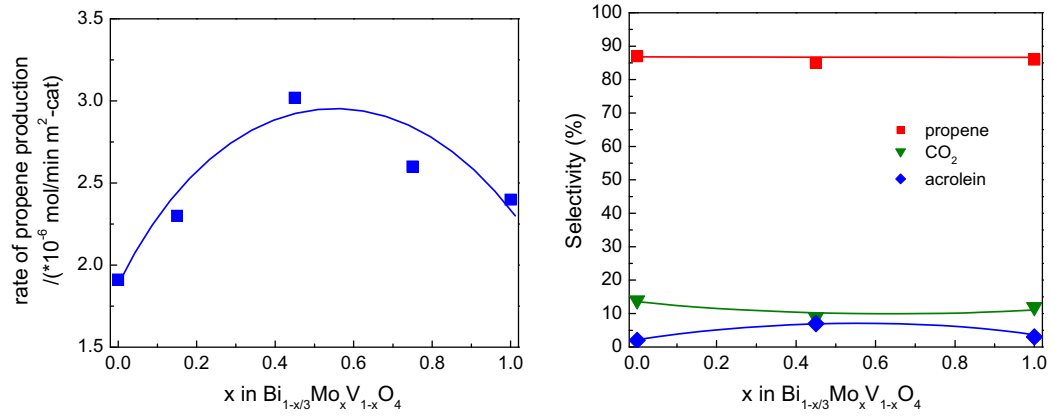

Fig. 5. Variation in the rate and selectivity of the oxidative dehydrogenation of propane to propene on $Bi_{1-x/3}V_{1-x}Mo_xO_4$ with *x*. For rate measurement total flow rate: 60 mL/min. P_{C3H8} = 0.067 atm, P_{O2} = 0.167 atm, 753 K.

Table 1
Reaction orders at different temperatures for the oxidation of 1-butene to produce 1,3-butadiene on $Bi_{1-x/3}V_{1-x}Mo_xO_4$. The partial pressures of 1-butene and oxygen were fixed at 0.067 and 0.167 atm when varying the other one.

Composition (*x*)	633 K		673 K		693 K	
	1-Butene	Oxygen	1-Butene	Oxygen	1-Butene	Oxygen
0	0.9 ± 0.0	0.0 ± 0.0	1.0 ± 0.0	−0.1 ± 0.1	0.9 ± 0.0	0.0 ± 0.0
0.45	0.1 ± 0.0	0.3 ± 0.0	0.9 ± 0.1	0.0 ± 0.1	1.0 ± 0.0	0.0 ± 0.1
1	0.8 ± 0.0	−0.1 ± 0.1	1.0 ± 0.0	−0.1 ± 0.1	0.9 ± 0.0	0.0 ± 0.0

Table 2
Reaction orders at different temperatures for trans-2-butene and oxygen to produce 1,3-butadiene on $Bi_{1-x/3}V_{1-x}Mo_xO_4$. The partial pressures of trans-2-butene and oxygen were fixed at 0.067 and 0.167 atm when varying the other one.

Composition (x)	633 K		673 K		693 K	
	Trans-2-butene	Oxygen	Trans-2-butene	Oxygen	Trans-2-butene	Oxygen
0	0.8 ± 0.1	0.2 ± 0.1	0.8 ± 0.1	0.2 ± 0.1	0.8 ± 0.1	0.3 ± 0.0
0.45	0.0 ± 0.1	0.3 ± 0.0	0.9 ± 0.0	0.1 ± 0.0	0.9 ± 0.1	0.1 ± 0.1
1	0.9 ± 0.0	0.0 ± 0.1	1.0 ± 0.1	0.0 ± 0.0	1.0 ± 0.0	0.2 ± 0.0

Table 3
Reaction orders at different temperatures for the oxidation of isobutene to produce methacrolein on $Bi_{1-x/3}V_{1-x}Mo_xO_4$. The partial pressures of isobutene and oxygen were fixed at 0.067 and 0.167 atm when varying the other one at 673 K (left). The partial pressures of isobutene and oxygen were fixed at 0.0167 atm and 0.167 atm when varying the other one at 703 K (right).

Composition (x)	673 K		703 K	
	Isobutene (0.05–0.15 atm)	Oxygen (0.067–0.167 atm)	Isobutene (<0.0167 atm)	Oxygen (0.067–0.167 atm)
0	0.9 ± 0.1	0.0 ± 0.1	1.0 ± 0.1	0.0 ± 0.1
0.45	−0.8 ± 0.1	0.8 ± 0.1	0.9 ± 0.2	0.0 ± 0.0
1	−0.9 ± 0.0	1.1 ± 0.1	0.9 ± 0.1	0.0 ± 0.0

Table 4
Reaction orders at different temperatures for the oxidative dehydrogenation of propane to produce propene on $Bi_{1-x/3}V_{1-x}Mo_xO_4$. The partial pressures of propane and oxygen were fixed at 0.067 and 0.167 atm when varying the other one at 773 K.

Composition (x)	773 K	
	Propane	Oxygen
0	1.0 ± 0.1	0.0 ± 0.0
0.45	1.1 ± 0.2	0.0 ± 0.1
1	1.0 ± 0.1	0.0 ± 0.0

3.1.3. Temperature dependence

Arrhenius plots for the oxidative dehydrogenation of 1-butene and trans-2-butene to 1,3-butadiene, the oxidation of isobutene to methacrolein, and the oxidative dehydrogenation of propane to propene over $Bi_{1-x/3}V_{1-x}Mo_xO_4$ are shown in Figs. 6–8 for temperature in the range of 613–773 K. Values of the apparent activation energies data are listed in Table 5–8.

For temperatures above 663 K, the apparent activation energies for 1-butene and trans-2-butene oxidative dehydrogenation to 1,3-butadiene increase slightly with x, from 6.5 to 9.2 kcal/mol for 1-butene oxidation, and from 14.0 to 17.4 kcal/mol for trans-2-butene oxidation. The activation energy for 1-butene oxidation to 1,3-butadiene obtained on bismuth molybdate (x = 1.0) is similar to that reported by Keizer et al. [41], 11 kcal/mol.

While the apparent activation energies for 1-butene and trans-2-butene oxidative dehydrogenation over $Bi_2Mo_3O_{12}$ and $BiVO_4$ are the same for temperatures below 663 K as they are for higher temperatures, for $Bi_{0.85}Mo_{0.45}V_{0.55}O_4$ the apparent activation energies below 663 K are higher than those measured at high temperatures, 24.3 kcal/mol in the case of 1-butene and 24.7 kcal/mol in the case of trans-2-butene. A similar pattern has been reported by Linn and Sleight [16] for 1-butene oxidation on bismuth molybdate, 14 kcal/mol for temperatures above 663 K, and 38 kcal/mol for temperatures below 663 K.

The apparent activation energy for the oxidation of isobutene to methacrolein exhibits a complex dependence upon the catalyst composition, the temperature regime, and the partial pressure of isobutene. For $BiVO_4$, the apparent activation energy is the same, 14.7 kcal/mol, independent of temperature or isobutene partial pressure in the feed (0.067 atm or 0.0167 atm). For $Bi_2Mo_3O_{12}$, the apparent activation energy is 21.6 kcal/mol when the isobutene partial pressure is 0.0167 atm and increases to 44.0 kcal/mol when the isobutene partial pressure is 0.067 atm, and for both

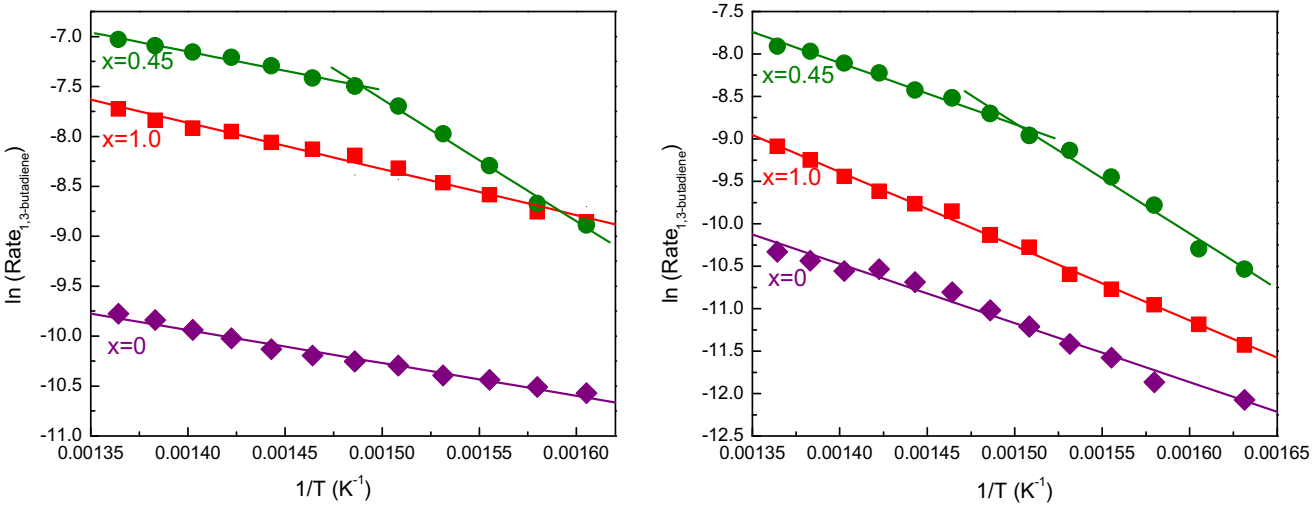

Fig. 6. Arrhenius plot of the oxidative dehydrogenation of 1-butene and trans-2-butene oxidation to 1,3-butadiene over $Bi_{1-x/3}V_{1-x}Mo_xO_4$ catalysts at 613–733 K. Left: 1-butene, P_{1-C4H8} = 0.067 atm, P_{O2} = 0.167 atm. Right: trans-2-butene, $P_{trans-2-C4H8}$ = 0.067 atm, P_{O2} = 0.167 atm. Total flow rate: 60 mL/min.

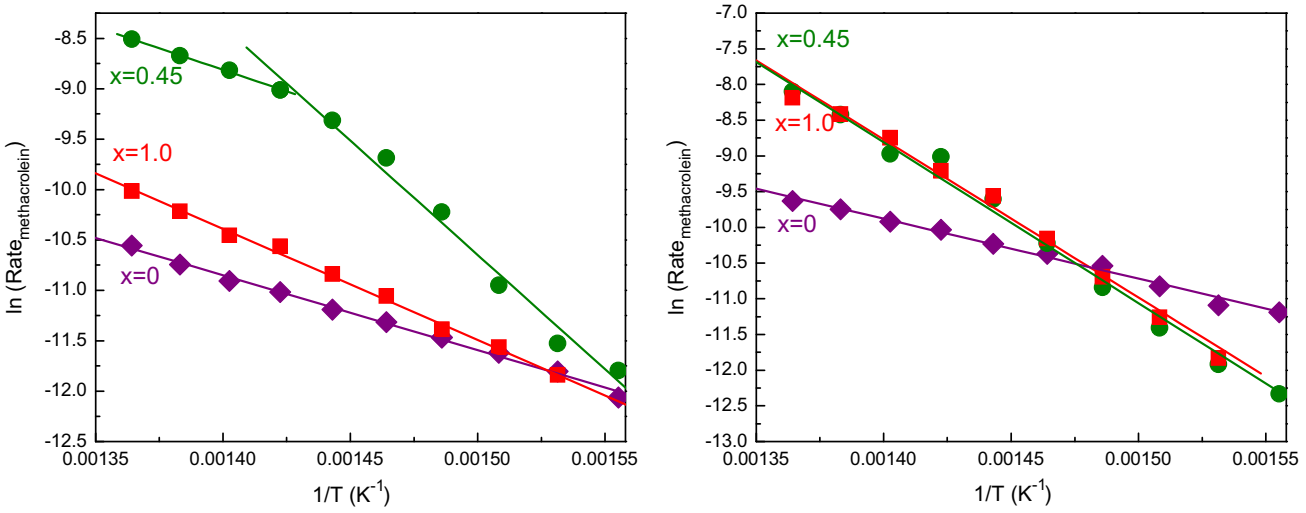

Fig. 7. Arrhenius plot of the isobutene oxidation to methacrolein over $Bi_{1-x/3}V_{1-x}Mo_xO_4$ catalysts at 613–733 K. Left: $P_{iso-C4H8}$ = 0.0167 atm, P_{O2} = 0.167 atm. Right: $P_{iso-C4H8}$ = 0.067 atm, P_{O2} = 0.167 atm. Total flow rate: 60 mL/min.

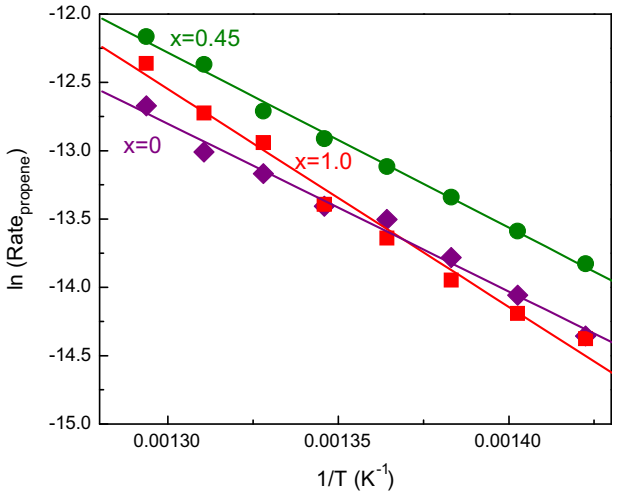

Fig. 8. Arrhenius plot of the oxidative dehydrogenation of propane to propene over $Bi_{1-x/3}V_{1-x}Mo_xO_4$ catalysts at 703–773 K and P_{C3H8} = 0.067 atm, P_{O2} = 0.167 atm. Total flow rate: 60 mL/min.

Table 5
Apparent activation energies under different temperature ranges for 1-butene and oxygen to produce 1,3-butadiene on $Bi_{1-x/3}V_{1-x}Mo_xO_4$. $P_{1\text{-}C4H8}$ = 0.067 atm, P_{O2} = 0.167 atm.

Composition (x)	E_{app} (kcal/mol)	
	663–713 K	613–663 K
0	6.5	6.5
0.45	7.6	24.3
1	9.2	9.2

isobutene partial pressures the apparent activation energy is independent of the temperature. In the case of $Bi_{0.85}Mo_{0.45}V_{0.55}O_4$, the apparent activation energy is found to depend on both the isobutene partial pressure and the reaction temperature. For an isobutene partial pressure of 0.0167 atm, the apparent activation energy is 17 kcal/mol for temperatures above 703 K and it is 44.0 kcal/mol for temperatures below 703 K. However, when the isobutene partial pressure is raised to 0.067 atm, the apparent activation energy becomes 44.0 kcal/mol independent of the reaction temperature (Fig. 7).

Table 6
Apparent activation energies under different temperature ranges for oxidation of trans-2-butene to produce 1,3-butadiene on $Bi_{1-x/3}V_{1-x}Mo_xO_4$. $P_{trans\text{-}2\text{-}C4H8}$ = 0.067 atm, P_{O2} = 0.167 atm.

Composition (x)	E_{app} (kcal/mol)	
	663–713 K	613–663 K
0	14.0	14.0
0.45	14.4	24.7
1	17.4	17.4

Table 7
Apparent activation energies under different temperature ranges for the oxidation of isobutene to methacrolein on $Bi_{1-x/3}V_{1-x}Mo_xO_4$. $P_{iso\text{-}C4H8}$ = 0.0167 atm, P_{O2} = 0.167 atm.

Composition (x)	E_{app} (kcal/mol)	
	703–733 K	643–703 K
0	14.7	14.7
0.45	17.0	44.8
1	21.6	21.6

Table 8
Apparent activation energies for the oxidative dehydrogenation of propane to propene on $Bi_{1-x/3}V_{1-x}Mo_xO_4$. P_{C3H8} = 0.167 atm, P_{O2} = 0.167 atm.

Composition (x)	E_{app} (kcal/mol)
	703–773 K
0	24.4
0.45	25.5
1	31.5

3.2. Catalyst characterization

XANES spectra were acquired in order to establish which elements are reduced at elevated temperature in the presence of different alkenes on $Bi_2Mo_3O_{12}$, $BiVO_4$, and $Bi_{0.85}Mo_{0.45}V_{0.55}O_4$. Measurements were taken before and after exposure to 1-butene, trans-2-butene, isobutene, and propene at 713 K for 2 h. All the spectra are shown in the Supplementary Information.

The position of the Bi L_3-edge did not change with time and remained identical to that for Bi_2O_3 independent of the

composition of the reducing agent or the catalyst compositions. After exposure to propene, 1-butene, trans-2-butene, and isobutene, the Mo K-edge shifted to lower energy, and the height of the pre-edge feature decreased. Similar trends were observed for the V K-edge. After reduction, the edge shifts and the pre-edge feature height decreased indicating a reduction of V. For both the Mo and V K-edges, a larger shift in the edge position and a smaller pre-edge feature were observed after reduction with all butene isomers than with propene, indicating that butenes are better reducing agents than propene. It is also noted that the reported changes in the Mo and V K-edge spectra were larger for $Bi_{0.85}V_{0.55}Mo_{0.45}O_4$ than for $BiVO_4$ or $Bi_2Mo_3O_{12}$.

Diffuse reflectance UV–VIS spectra were acquired in order to further characterize the reducing power of different butenes. When the catalyst is heated to 673 K and exposed to a reducing agent, the absorbance of the baseline at a wave number below the adsorption edge increased as a function of time, due to catalyst reduction. The absorbance at 800 nm was plotted as a function of time of exposure to reducing conditions, and the initial reduction rate was calculated (Supplementary Information). The correlation of the apparent rate coefficient k_{app} for different butene isomers with the initial rate of reduction measured by UV–VIS on $Bi_{0.85}V_{0.55}Mo_{0.45}O_4$ is shown in Fig. 9. The observed linear correlation suggests that the oxidation of alkenes proceeds via a Mars van Krevelen mechanism involving catalyst oxygen atoms. The more readily the reactant can be reduced, the higher is the reaction rate. The reducibility of isobutene and trans-2-butene is lower than that of 1-butene, but greater than that of propene.

4. Discussion

4.1. Mechanism and kinetics of the oxidative dehydrogenation of propane, 1-butene, and trans-2-butene, and oxidation of isobutene

Tables 1 and 2 show that the kinetics for the oxidative dehydrogenation of propane to propene and of 1-butene and trans-2-butene to butadiene are very similar—essentially first order in the partial pressure of the alkane or alkene and zero order in the partial pressure of oxygen—for $BiVO_4$ and Bi_2MoO_{12}, and for $Bi_{0.85}V_{0.55}Mo_{0.45}O_4$ at temperatures above 663 K. Taken together, the UV–Vis and XANES data presented in Fig. 9 and Figs. S1–S5 (Supplementary Information) suggest that in all cases oxidative dehydrogenation proceeds via a Mars van Krevelen mechanism involving oxygen atoms of the catalysts. The observed kinetics can be rationalized on the basis of the mechanism shown in Scheme 1, which is illustrated for the oxidative dehydrogenation of 1-butene on Bi_2MoO_{12} and is similar to that developed to explain the kinetics of propene oxidation to acrolein [37]. Reaction begins with the physical adsorption of 1-butene (Step 1) followed by hydrogen abstraction from the —CH_2— group of 1-butene by one of the Mo=O bonds of the catalyst and concurrent reduction of Mo^{6+} to Mo^{5+} (Step 2). As in the case for propene oxidation, Step 2 is taken to be the rate-limiting step. Hydrogen abstraction is taken to occur from the —CH_2— group of 1-butene because the strength of this C—H bond is weaker than that of other C—H bonds in the reactant. As discussed below, this assumption is supported by the observation that the apparent activation energy for the oxidative dehydrogenation of propane, 1-butene, and trans-2-butene correlates with the strength of the weakest C—H bond of the reactant. Getsoian et al. [38,39] have demonstrated that of the three types of Mo=O bonds present on the surface of Bi_2MoO_{12}, and the one that weakly interacts with the lone pair on Bi (e.g., Bi···O=Mo) is the most active for activating the C—H bond in the methyl group of propene. We, therefore, assume that this will also be the most active form of oxygen in the present system. The next step following C—H bond cleavage of the reactant involves abstraction of a hydrogen atom from the methyl group of the methyl-allyl radical (Step 3), which reduces the adjacent Mo=O to Mo^{5+} and produces 1,3-butadiene. In the final two steps of the cycle, water is formed and desorbed reversibly producing two oxygen vacancies (Step 4) and the catalyst is then reoxidized by oxygen.

A rate expression for the rate of 1-butene consumption shown in Eq. (3) can be derived under the assumption that Step 2 is rate-limiting and that the pseudo-steady-state assumption is valid for intermediates [37]:

$$\text{rate} = \frac{k_1 k_2 P_{C_4H_8}[S]}{(k_2 + k_{-1})\left[1 + \frac{k_1 P_{C_4H_8}}{k_2 + k_{-1}} + \frac{k_1 k_2 P_{C_4H_8}}{k_3(k_2 + k_{-1})} + \left(\frac{k_1 k_2 P_{C_4H_8}}{k_4(k_2 + k_{-1})} + \frac{k_1 k_2 k_{-4} P_{C_4H_8} P_{H_2O}}{k_4 k_5 P_{O_2}(k_2 + k_{-1})}\right) + \frac{k_1 k_2 P_{C_4H_8}}{k_5 P_{O_2}(k_2 + k_{-1})}\right]} \quad (3)$$

In Eq. (3), k_i and k_{-i} represent the rate coefficients for reaction i in the forward and reverse directions, respectively, K_i represents the equilibrium constant for reaction i, P_j represents the partial pressure of reactant or product j, and [S] is the number of active sites per unit BET catalyst surface area.

When the rate of catalyst reoxidation is rapid relative to the rate of catalyst reduction, catalyst surface is fully oxidized, and if it is assumed that $k_{-1} \gg k_2$, then Eq. (3) simplifies to

$$\text{rate} = \frac{k_1 k_2 [S]}{(k_{-1} + k_2)} P_{C_4H_8} \cong K_1 k_2 P_{C_4H_8}[S] = k_{app} P_{C_4H_8} \quad (4)$$

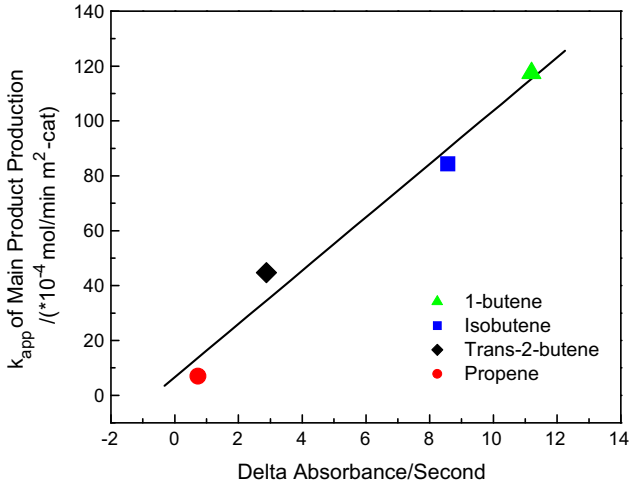

Fig. 9. Correlation of the apparent rate coefficient for the production of the principle product, k_{app}, at 703 K for different butene isomers (P_{C4H8} = 0.0167, P_{O2} = 0.167 atm) and initial rate of reduction measured using UV–VIS at 703 K (P_{C4H8} = 0.0167 atm) on $Bi_{0.85}V_{0.55}Mo_{0.45}O_4$.

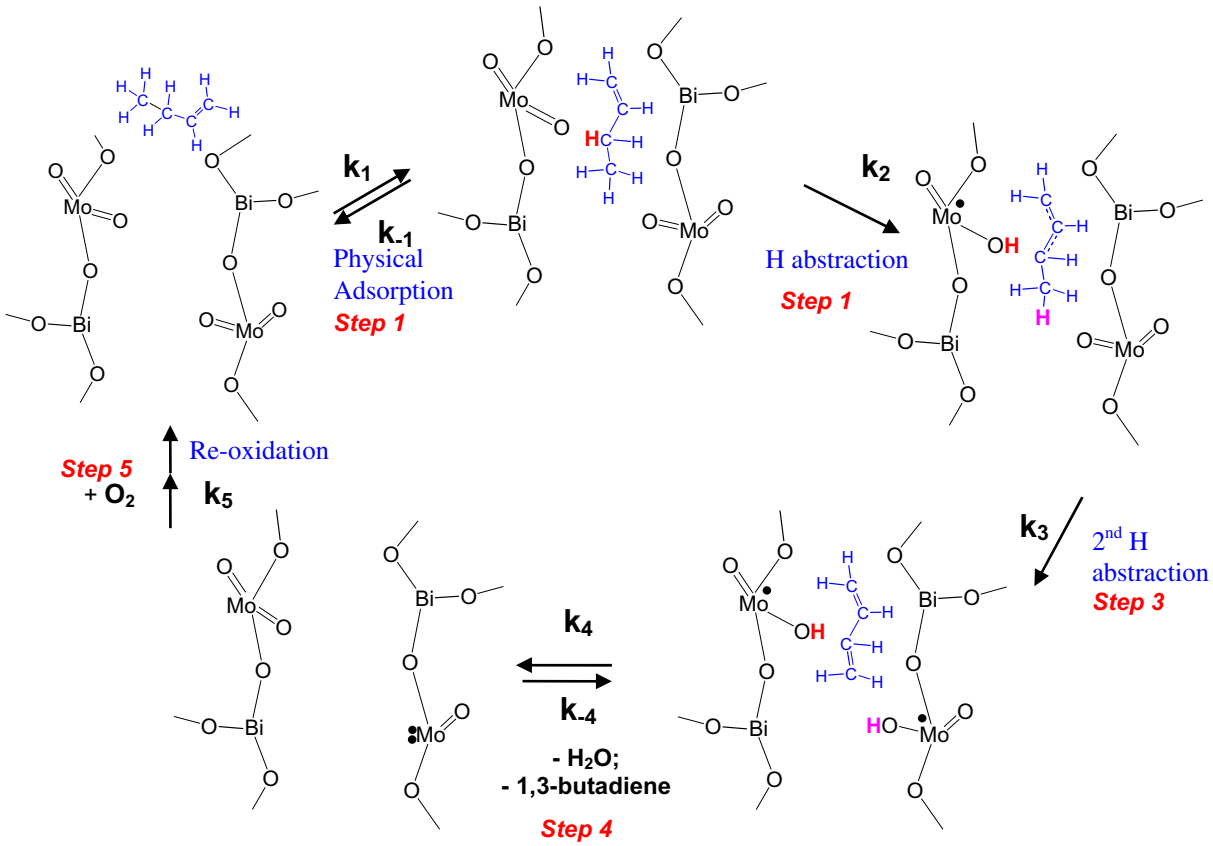

Scheme 1. The mechanism of the oxidative dehydrogenation of 1-butene to 1,3-butadiene over $Bi_2Mo_3O_{12}$ proposed on the basis of data reported in this study.

and the apparent rate constant k_{app} is now given by $K_1k_2[S]$. The form of Eq. (4) is completely consistent with the kinetics observed for the oxidative dehydrogenation of 1-butene and trans-2-butene on $BiVO_4$ and Bi_2MoO_{12} at all temperatures and for $Bi_{0.85}V_{0.55}Mo_{0.45}O_4$ at temperatures above 663 K. It is also noted that Eq. (4) also holds for the oxidative dehydrogenation of propane at all temperatures for all three catalysts ($BiVO_4$, $Bi_{0.85}V_{0.55}Mo_{0.45}O_4$, and Bi_2MoO_{12}).

Tables 1 and 2 show that for $Bi_{0.85}V_{0.55}Mo_{0.45}O_4$ the orders in 1-butene and trans-2-butene change significantly for temperatures below 663 K. Thus, at 633 K, the order in alkene decreases to nearly zero and the order in oxygen rises to 0.3. We also note that the apparent activation energy increases for both isomers of butene. Notably, though, changes in reaction order in alkene and oxygen, and the apparent activation energy, do not change for the oxidative dehydrogenation of propane to propene over $Bi_{0.85}V_{0.55}Mo_{0.45}O_4$. We attribute the changes in the reaction orders and the apparent activation energy to a transition of the catalyst from a state in which the catalyst surface is fully saturated with oxygen to one in which the catalyst is partially reduced. Under the latter circumstance, the rate of catalyst reoxidation becomes rate limiting. The reason that the transition in kinetic regimes is not observed for the oxidative dehydrogenation of propane is that the rate of this reaction is two orders of magnitude lower than that for oxidative dehydrogenation of either 1-butene or 2-butene. Reference to Eq. (3) shows that in the limit that the ratio of k_2/k_5 becomes very large, the last term in the denominator becomes dominant and the rate expression reduces to

$$\text{rate} = k_5 P_{O_2} \tag{5}$$

The kinetics for isobutene oxidation to methacrolein for temperatures above 663 K are very similar to those reported earlier for the oxidation of propene to acrolein, to the kinetics reported here for the oxidative dehydrogenation of 1-butene and trans-2-butene to 1,3-butadiene, and the kinetics for the oxidative dehydrogenation of propane to propene. For $BiVO_4$, the kinetics are first order in isobutene and zero order in oxygen independent of the isobutene partial pressure (0.0167 atm or 0.067 atm) and for Bi_2MoO_{12} and $Bi_{0.85}V_{0.55}Mo_{0.45}O_4$ only for isobutene partial pressures below 0.0167 atm. We note that under these constraints the apparent activation energies for isobutene oxidation are 14.7 kcal/mol for $BiVO_4$, 17.0 kcal/mol for Bi_2MoO_{12}, and 21.6 kcal/mol for $Bi_{0.85}V_{0.55}Mo_{0.45}O_4$.

The kinetics of isobutene oxidation have been discussed to only a limited degree, with very different conclusions drawn by different authors [31–33]. Mann and Ko [31] considered 13 different mechanisms, and concluded rate of reaction on copper-promoted bismuth molybdate is described best by a mechanism in which the rate-controlling step is assumed to be the surface reaction between charged absorbed 2-methylpropene and oxygen molecules. By contrast, Benyahia and Mearns [32,33] found fractional apparent orders with respect to isobutene and oxygen for isobutene oxidation over multicomponent bismuth molybdate, which they rationalized on the basis of a redox model. It should be noted though none of these studies reported sufficient rate data and catalyst characterization from which one could develop a compelling case for a particular reaction mechanism.

The kinetics of isobutene oxidation for the conditions noted above can be rationalized using the mechanism proposed in Scheme 2, which is very similar to that reported in our earlier work on the oxidation of propene to acrolein [37], as well as being similar to that shown in Scheme 1 for the oxidative dehydrogenation of alkenes and alkanes. The primary difference is that the 2-methyl-allyl radical formed in Step 2 is now trapped by reaction with a molybdenyl oxygen atom. This step, in turn, leads to the formation of methacrolein. By contrast, the 1-methyl-allyl radical formed

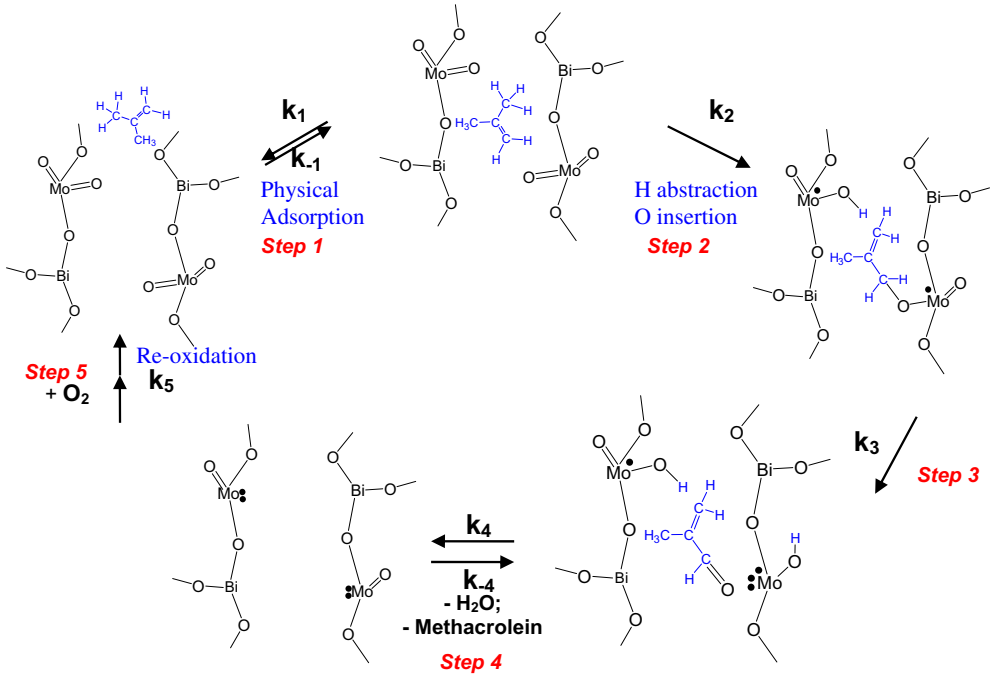

Scheme 2. The mechanism of the oxidation isobutene to methacrolein over $Bi_2Mo_3O_{12}$ under lower partial pressure of isobutene proposed on the basis of data reported in this study.

from 1-butene or trans-2-butene is not stabilized and instead loses an H atom to form 1,3-butadiene. Moro-oka has noted that oxygen addition is only observed when the intermediate formed upon cleavage of the weakest C—H bond of the reactant does not have a weak C—H bond that can be easily cleaved [42]. In accord with Moro-oka's statement, we note that the C—H bond in the methyl group of 1-methyl-allyl will cleave easily leading to the formation of 1,3-butadiene. However, the C—H bond in the methyl group of 2-methyl-allyl is harder to cleave and consequently is not possible to form a stable product. As a result, 2-methyl-allyl (from isobutene) will undergo oxygen insertion to form methacrolein, but 1-methyl-allyl (from 1-butene and trans-2-butene) will form 1,3-butadiene directly after dehydrogenation.

As noted earlier, the kinetics of isobutene are significantly different for Bi_2MoO_{12} and $Bi_{0.85}V_{0.55}Mo_{0.45}O_4$ for high isobutene partial pressures, and in the case of $Bi_{0.85}V_{0.55}Mo_{0.45}O_4$ at temperatures below 703 K. Under these conditions, the isobutene partial pressure becomes inverse first order and the oxygen partial pressure becomes first order, and the apparent activation energy increases to 44 kcal/mol for both catalysts. In situ UV–Vis spectra (see Supporting Information) also show more significant reduction of $Bi_{0.85}V_{0.55}Mo_{0.45}O_4$ at 673 K particularly for an isobutene partial

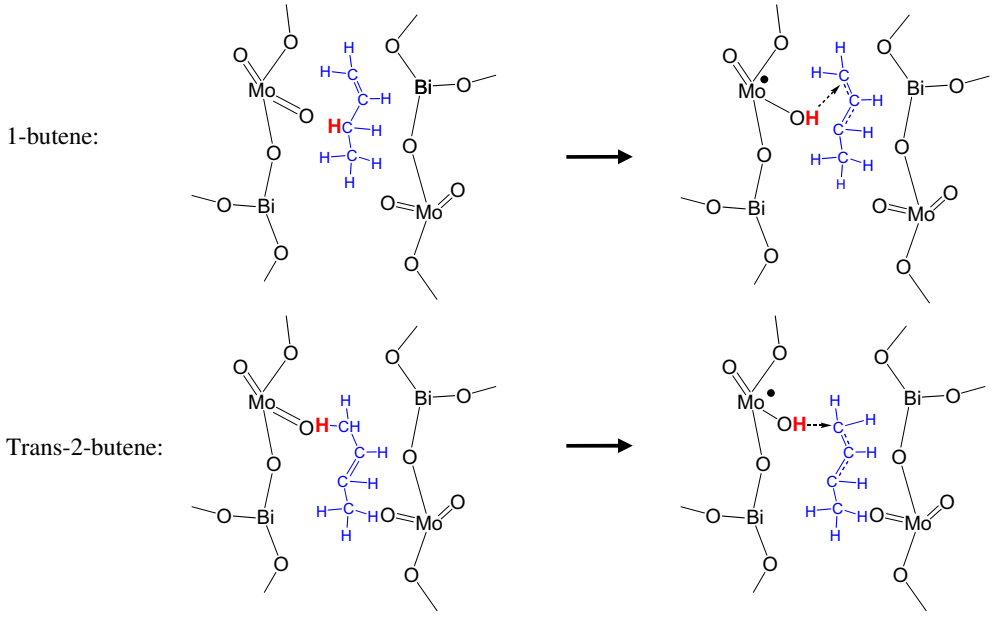

Scheme 3. Differences in the mechanisms of isomers formation from 1-butene and trans-2-butene.

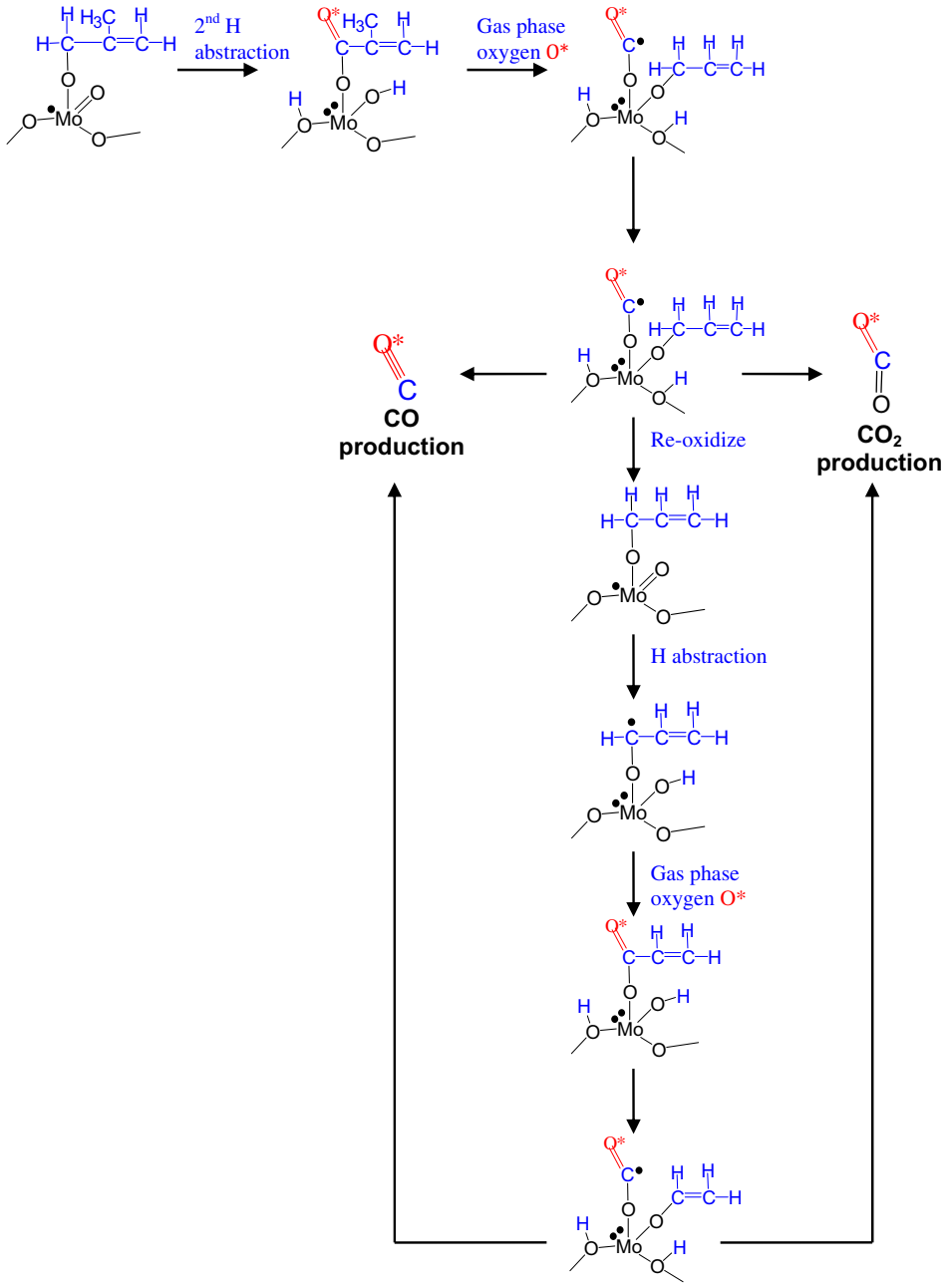

Scheme 4. Possible pathway for CO and CO_2 formation on $Bi_2Mo_3O_{12}$ during isobutene oxidation.

Table 9
Symmetry number (σ) for different reactants.

Reactant	Symmetry number (σ)
Propene	3
1-Butene	2
Trans-2-butene	6
Isobutene	6
Propane	6

pressure of 0.067 atm than is observed the same experiment is carried out in 1-butene. Visual inspection of the catalyst after operation under steady-state reaction conditions also confirms that isobutene reduces both Bi_2MoO_{12} and $Bi_{0.85}V_{0.55}Mo_{0.45}O_4$ to a greater extent than does 1-butene. After reaction in 0.067 atm of isobutene and 0.167 atm of oxygen, the color of Bi_2MoO_{12} changes from white for the fully oxidized catalyst to gray, and $Bi_{0.85}V_{0.55}Mo_{0.45}O_4$ changes from bright yellow to dark yellow.

The kinetics of isobutene oxidation observed on the reduced forms of Bi_2MoO_{12} and $Bi_{0.85}V_{0.55}Mo_{0.45}O_4$ can be rationalized in terms of the following reactions sequence:

$$(1)\ * + \text{iso-}C_4H_8 \overset{K1}{\longleftrightarrow} \text{piso-}C_4H_8*$$

$$(2)\ * + O_2 \overset{K2}{\longleftrightarrow} O_2*$$

$$(3)\ \text{iso-}C_4H_8* + O_2* \overset{k3}{\longrightarrow} C_4H_6O* + H_2O*$$

$$(4)\ C_4H_6O* \overset{K4}{\longleftrightarrow} C_4H_6O + *$$

$$(5)\ H_2O* \overset{K5}{\longleftrightarrow} H_2O + *$$

where "*" represents an active site. In contrast to the mechanism presented in Scheme 2, it is assumed here that oxidation occurs via reaction with adsorbed O_2. Implicit in the development of this

pathway is that the reduction of the catalyst is much more rapid than its reoxidation. Step 1 and Step 2 of the proposed sequence represent the adsorption of isobutene and oxygen onto active sites. Step 3 is the bimolecular reaction of the adsorbed molecules. Steps 4 and 5 are desorption of methacrolein and water. If Steps 1, 2, 4, and 5 are assumed to be quasi-equilibrated and Step 3 is the irreversible, rate-determining step, then the rate of methacrolein formation is given by the following relation:

$$\text{rate}_{\text{methacrolein}} = \frac{k_3 K_1 K_2 P_{\text{iso-C}_4\text{H}_8} P_{\text{O}_2}[S]}{\left(1 + K_1 P_{\text{iso-C}_4\text{H}_8} + K_2 P_{\text{O}_2} + \frac{P_{\text{C}_4\text{H}_6\text{O}}}{K_4} + \frac{P_{\text{H}_2\text{O}}}{K_5}\right)^2} \quad (6)$$

Since the conversion of isobutene was always below 5%, we assume that $P_{\text{C}_4\text{H}_6\text{O}}$ and $P_{\text{H}_2\text{O}}$ are negligible. If we assume that at higher isobutene partial pressures, isobutene is strongly adsorbed onto the catalyst surface, so that adsorbed isobutene is the most abundant surface intermediate, then

$$\text{rate}_{\text{methacrolein}} = \frac{k_3 K_2 P_{\text{O}_2}[S]}{P_{\text{iso-C}_4\text{H}_8}} \quad (7)$$

Eq. (7) is consistent with the observed kinetics shown in Table 3, in which the rate of isobutene oxidation to methacrolein is negative first order in isobutene and positive first order in oxygen. This rate expression suggests that the high apparent activation energy measure for reduced Bi_2MoO_{12} and $Bi_{0.85}V_{0.55}Mo_{0.45}O_4$ is attributable to an even higher activation barrier for Step 3.

To this point, we have only discussed the mechanism and kinetics for formation of primary products. Therefore, we turn next to a discussion of the mechanism by which by-products are formed. The by-products of 1-butene and trans-2-butene over $Bi_{1-x/3}V_{1-x}Mo_xO_4$ catalysts are other butene isomers, but the by-products of isobutene are mainly CO, CO_2, and ethene.

For the oxidative dehydrogenation of 1-butene and trans-2-butene, once the 1-methyl-allyl intermediate is formed following H abstraction, the intermediate can undergo further hydrogen abstraction, yielding 1,3-butadiene, or reinsertion of the first abstracted hydrogen at the end of the allylic moiety to yield other isomers. One might expect this process to lead to the same product distribution regardless of the starting alkene. However, our experimental data show that the product distributions resulting from the allylic intermediates produced from 1-butene and trans-2-butene are different (Fig. 2). The selectivity to 1,3-butadiene is higher than that for 1-butene compared to trans-2-butene, indicating oxidative dehydrogenation is favored for 1-butene, but isomerization is favored for trans-2-butene. Similar results have been observed by Portela [8], and the reason can be explained as follows. For 1-butene, once 1-methyl-allyl intermediate is formed, the insertion must occur at the end of the intermediate. However, the position of the first abstracted hydrogen is not at the end of the intermediate. For trans-2-butene, the position of the first abstracted hydrogen is at the end of the intermediate, so it becomes much easier to form an isomerization product, cis-2-butene. This difference is illustrated in Scheme 3. The proposed pathways also help to explain the higher selectivity to cis-2-butene than 1-butene from trans-2-butene.

The by-product formation occurring during the oxidation of isobutene is different from that observed for 1- and trans-2-butene. Isobutene does not undergo isomerization because the structure of the 2-methyl-allyl intermediate does not lend itself to isomerization, and thus only CO and CO_2 are formed as by-products. The partial pressure dependence on O_2 for CO_2 formation is 0.4

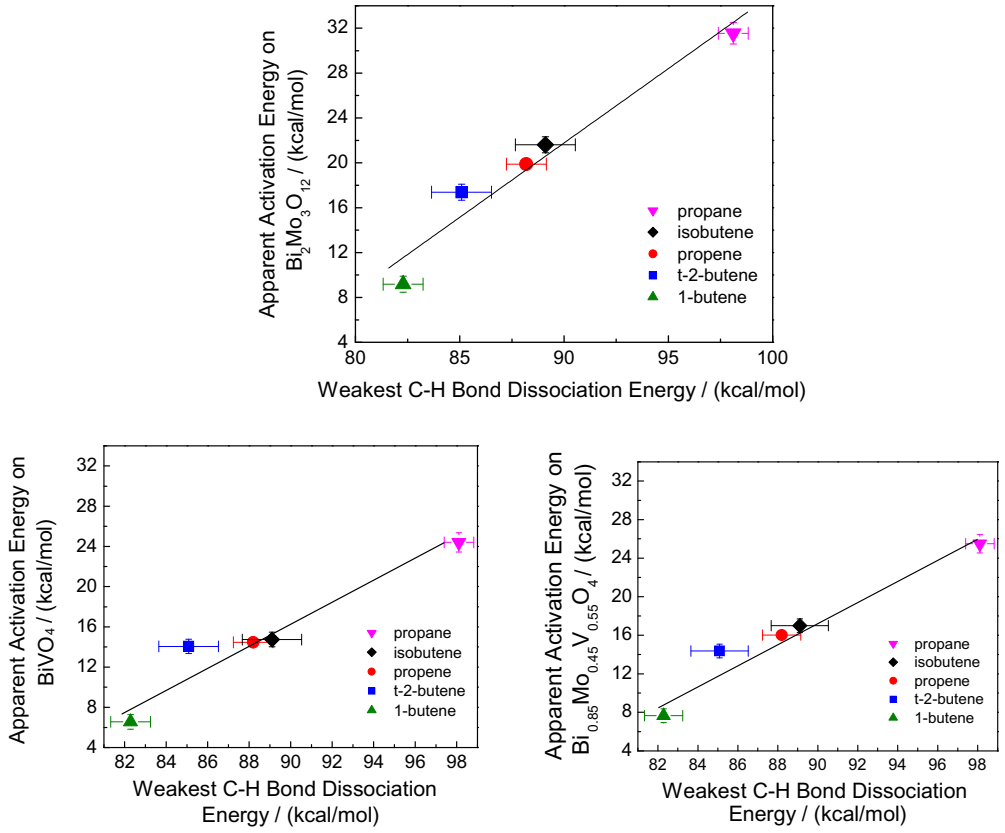

Fig. 10. Correlation of the apparent activation energy for formation of the principle product with the dissociation energy of the weakest C—H bond involved in the rate-determining step occurring on $Bi_2Mo_3O_{12}$ (top), $BiVO_4$ (bottom left), and $Bi_{0.85}V_{0.55}Mo_{0.45}O_4$ (bottom right). All bond dissociation energy data come from: Handbook of bond dissociation energies in organic compounds. Yu-Ran Luo. CRC Press, 2003.

on $Bi_2Mo_3O_{12}$ and is first order for CO formation, which is the same as for propene oxidation. This suggests that the oxygen atoms in CO_2 come from both gas phase oxygen and lattice oxygen; however, the oxygen atom in CO only comes from gas phase oxygen. Possible pathways to these products are shown in Scheme 4. We still assume that CO and CO_2 originate from the precursor to methacrolein, in a manner similar to what we proposed earlier for CO and CO_2 formation from propene. However, since the selectivity of methacrolein from isobutene is lower (~50%, Fig. 3) than the selectivity of acrolein from propene (~70%) [37] on bismuth molybdate, the selectivities to CO and CO_2 are higher for isobutene than for propene. As is shown in Scheme 4, for isobutene, the reaction sequence begins with the 2-methyl-allyl species formed in the rate-limiting step. Reaction of adsorbed O_2 with this species is proposed to form an intermediate leading to CO and CO_2. After re-oxidization, a new intermediate is formed, which can also produce CO and CO_2. This intermediate is exactly the same as the starting point of the allyl species formed in the RDS for propene to acrolein [37]. As a result, one isobutene molecule can produce more CO and CO_2 than propene, leading to a higher selectivity of CO and CO_2. In this mechanism, the oxygen in CO comes from O_2, whereas in CO_2 one of the oxygen atoms comes from O_2 and the other from lattice oxygen.

4.2. Correlation of the apparent activation energies and pre-exponential factors with the molecular structure of the reactants

The discussion of the mechanism and kinetics for the oxidative dehydrogenation of propane, 1-butene, and trans-2-butene and for the oxidation of isobutene is very similar at temperatures above 673 K, for which the catalyst is saturated with oxygen and the rate-limiting step is assumed to involve cleavage of the weakest C—H bond in the reactant. As noted earlier, under these circumstances, the rate of alkane of alkene consumption can be described by Eq. (4). This expression can now be written to identify the significance of the apparent pre-exponential factor and the apparent activation barrier. Thus

$$k_{app} = K_1 k_2 [S] = \sigma A_{app} \exp\left(\frac{-E_{app}}{RT}\right)[S] = \sigma A_{app} \exp\left(\frac{-\Delta H_{ads} - E_{int}}{RT}\right)[S] \quad (8)$$

where σ is the symmetry number (i.e., how many equivalent C—H bonds could participate in the rate-limiting step). The symmetry number for different reactants is shown in Table 9. The apparent activation energy is the sum of the change in enthalpy of the adsorbate upon adsorption of a hydrocarbon molecule onto the surface, ΔH_{ads}, and the intrinsic activation energy of the C—H bond breaking, E_{int}. If we assume that the heat of adsorption is similar for all the butene isomers, and the difference between propene and 1-butene on bismuth molybdate is ~3 kcal/mol [43], we can expect a similar positive correlation between the intrinsic activation energy and the weakest C—H bond dissociation energy. The stronger the C—H bond, the more energy is needed to break it. We, therefore, conclude that a plausible descriptor for relating reactant activity is the strength of the weakest C—H bond.

Based on the preceding discussion, we plot the apparent activation energy versus the weakest C—H bond dissociation energy measure for the oxidative dehydrogenation of propane, 1-butene, and trans-2-butene, and for the oxidation of propene [37] and isobutene carried out over $Bi_2Mo_3O_{12}$, $Bi_{0.85}V_{0.55}Mo_{0.45}O_4$, and on

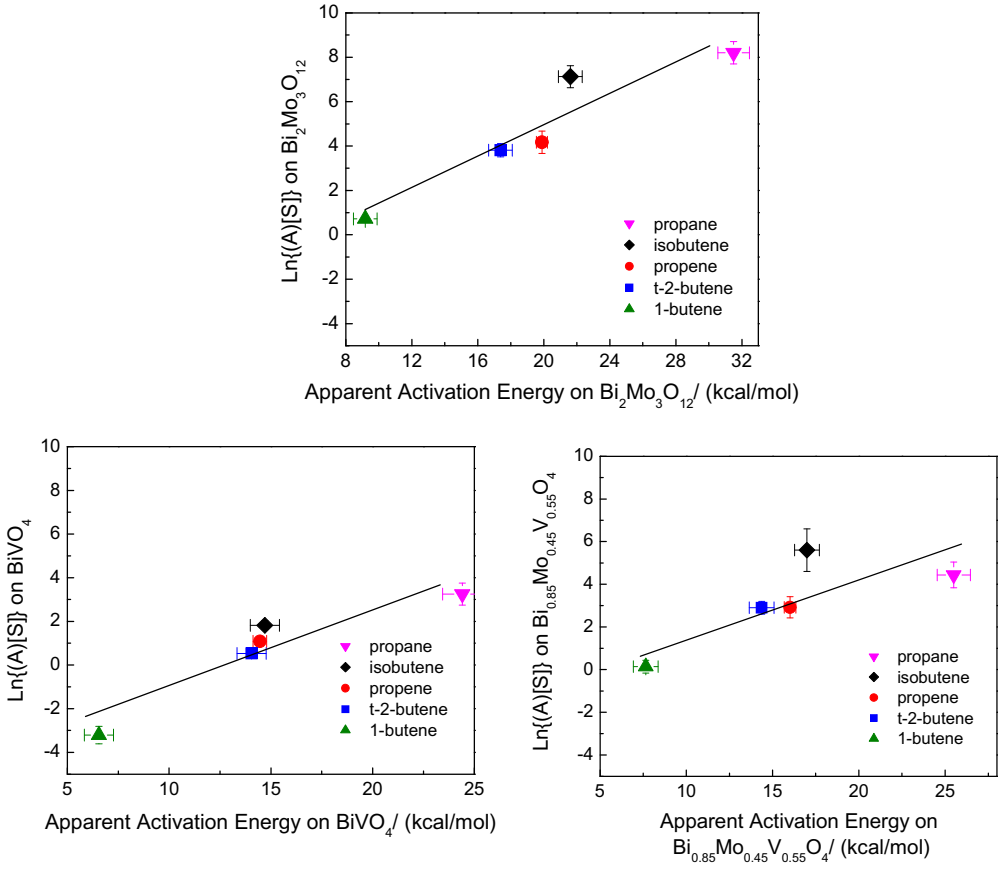

Fig. 11. Correlation of the natural log of apparent pre-exponential factor with the apparent activation energy for formation of the principle products occurring over $Bi_2Mo_3O_{12}$ (top), $BiVO_4$ (bottom left), and $Bi_{0.85}V_{0.55}Mo_{0.45}O_4$ (bottom right).

$BiVO_4$. Fig. 10 shows that for reactions over a given metal oxide, the apparent activation energy correlates with the strength of the weakest C—H bond. We note that the observed correlation is consistent with the theoretical interpretation of the intrinsic activation energy developed by Getsoian et al. for the oxidation of propene to acrolein [44]. The authors of this study reported that the intrinsic activation energy (E_{int}) determined from density functional theory can be interpreted in terms of the following sum:

$$E_{int} = E_{C-H} + E_G + E_{O-H} \quad (9)$$

in which E_{C-H}, E_{O-H}, and E_G refer to the energy required for dissociation of a C—H bond, formation of an O—H bond, and the band gap of the catalyst, respectively.

For a given reactant, the bond dissociation energy of the C—H bond involved in the rate-limiting step is the same and independent of catalyst composition. The DFT calculations suggest that the O—H bond formation energy does not depend strongly on the identity of the nearest neighbor to oxygen, leading to the conclusion that the principle term in Eq. (9) depending on catalyst composition is E_G, and hence, that for a given value of E_{C-H}, the apparent activation energy should increase with this parameter. A correlation of E_{int} with E_G for propene oxidation to acrolein was reported by Getsoian et al. [44] A similar trend can be deduced from Fig. 10, consistent with the decrease in the measured band gap in the order $Bi_2Mo_3O_{12}$ (2.70 eV) > $Bi_{0.85}V_{0.55}Mo_{0.45}O_4$ (2.32 eV) > $BiVO_4$ (2.06 eV).

The next question is whether the apparent pre-exponential factor, A_{app}, correlates with the apparent activation energy. This question is difficult to address unambiguously because it is not known whether the number of active sites, [S], is constant with changes in catalyst composition. For this reason, Fig. 11 shows plots of $\ln(A_{app}[S])$ versus E_{app} for three representative catalysts, since it is reasonable to assume that the number of active sites for a given catalyst composition is independent of the composition of the reactant. It is evident from Fig. 11 that for each catalyst there is a positive correlation between $\ln(A_{app}[S])$ and E_{app}. It is notable that the data points for isobutene oxidation lie farthest from the trend line and always above this line. Although the reason for this deviation is not known, we hypothesize that nature of the deviation suggests that the isobutene may access a larger number of surface oxygen atoms than that can any of the other reactants. This interpretation is certainly qualitatively consistent with the observation that isobutene is a more effective reducing agent than 1-butene or trans-2-butene.

The positive correlation of A_{app} with E_{app} indicates that the product of the pre-exponential factor for k_2 and entropy term of adsorption for K_1 in Eq. (8) increases with the activation energy for this reaction. While it is possible that changes in the entropy of adsorption also contribute to changes in the magnitude of A_{app}, this seems unlikely, since the values for E_{app} and A_{app} are very similar for both propene oxidation and butene oxidative dehydrogenation. We, therefore, suggest that the principle cause of the increases in A_{app} is attributable to increase in the activation entropy for Step 2. This trend is what would be expected for a looser transition state involving a higher activation barrier.

5. Conclusions

The oxidative dehydrogenation of 1-butene and trans-2-butene to 1,3-butadiene, the oxidative dehydrogenation of propane to propene, and the oxidation of isobutene to methacrolein were investigated over $Bi_{1-x/3}V_{1-x}Mo_xO_4$ for a range of temperatures and reactant partial pressures. These investigations were complemented by characterization of the oxidation state of the catalyst by XANES and UV–Vis spectroscopy. These studies show that the reaction kinetics are strongly dependent on the state of catalyst reduction, which in turn depends on the catalyst and reactant composition, and on the reaction temperature and reactant partial pressures.

For conditions where the catalyst is fully oxidized state, the kinetics of all reactions are nearly identical. The rate of reaction is linearly dependent on the alkane or alkene partial pressure and independent of the oxygen partial pressure, and the apparent activation energy ranges from 6.5 kcal/mol to 31.5 kcal/mol depending on the reactant composition. The kinetics for oxidative dehydrogenation and oxidation over fully oxidized catalysts can be interpreted in terms of a Mars van Krevelen mechanism in which the reactant adsorbs reversibly on the catalyst surface and then undergoes cleavage of the weakest C—H bond in the rate-limiting step. In the case of 1-butene and trans-2-butene, the allyl radical formed contains a relatively weak C—H bond which can undergo cleavage leading to 1,3-butadiene. By contrast, the allyl radical formed from isobutene does not contain such a C—H bond and instead is first stabilized by addition to an oxygen atom on the catalyst surface. Subsequent cleavage of an H atom from the α-carbon atom of the vinyl alkoxide intermediate leads to the formation of methacrolein. This pattern of reaction is similar to that observed previously for the oxidation of propene to acrolein [37]. The apparent activation energy and pre-exponential factors for both the oxidative dehydrogenation of propane, 1-butene, and trans-2-butene, and for the oxidation of propene and isobutene increase with the strength of the weakest C—H bond of the reactant involved in the rate-limiting step. A correlation of the apparent pre-exponential factor with the apparent activation energy, and hence the weakest C—H bond of the reactant is also observed. It is proposed that this trend is attributable to a transition state structure that is more strongly bound to the catalyst surface and is more negative in entropy change the stronger is the C—H bond that must be cleaved. For a given reactant, it is also observed that the lower the apparent activation energy is the lower the band gap of the catalyst, and hence, it eases of undergoing reduction.

A second regime is observed when the catalyst cannot be maintained in a fully oxidized state, and the rate of reaction becomes rate-limited by the reoxidation of the catalysts. This is the case for the oxidative dehydrogenation of 1- and trans-2-butene over $Bi_{0.85}V_{0.55}Mo_{0.45}O_4$ at low-temperature regime. In this case, the rate of oxidative dehydrogenation becomes zero order in alkene partial pressure and fractional oxygen partial pressure, and the apparent activation energy becomes independent of reactant composition.

A third reaction regime is observed for isobutene oxidation under conditions that result in a substantial degree of catalyst reduction. For $Bi_2Mo_3O_{12}$ and $Bi_{0.85}Mo_{0.45}V_{0.55}O_4$, the activation energy is 44.0 kcal/mol at all temperatures when the isobutene partial pressure is raised to 0.067 atm. This same apparent activation energy is observed for $Bi_{0.85}Mo_{0.45}V_{0.55}O_4$ at temperatures below 703 K when the isobutene partial pressure is 0.0167 atm.

Acknowledgments

This work was funded by Director, Office of Science, Office of Basic Energy Sciences of the U.S. Department of Energy under Contract No. DE-AC02-05CH11231. Portions of this research were carried out at the Argonne National Laboratory (ANL), managed by the University of Chicago-Argonne, LLC, for the U.S. Department of Energy, Office of Science.

Appendix A. Supplementary material

Supplementary data associated with this article can be found, in the online version, at http://dx.doi.org/10.1016/j.jcat.2015.02.015.

References

[1] J.D. Idol, U.S. Patent 2, 904, 580, 1959.
[2] G.W. Hearne, M.L. Adams, U.S. Patent 2, 451, 485 1948.
[3] P.H.A. Batist, J.F.H. Bouwens, G.C.A. Schuit, J. Catal. 25 (1972) 1–11.
[4] J.M. Lopez Nieto, E.A. Burga, G. Kremenic, Ind. Eng. Chem. Res. 29 (1990) 337–342.
[5] S. Breiter, H.-G. Lintz, Chem. Eng. Sci. 50 (1995) 785–791.
[6] H. Lee, J.C. Jung, H. Kim, Y.-M. Chung, T.J. Kim, S.J. Lee, S.-H. Oh, Y.S. Kim, I.K. Song, Catal. Commun. 9 (2008) 1137–1172.
[7] D.A.G. van Oeffelen, J.H.C. van Hooff, G.C.A. Schuit, J. Catal. 95 (1985) 84–100.
[8] M. Farinha Portela, Top. Catal. 15 (2001) 241–243.
[9] H.H. Voge, C.D. Wagner, D.P. Setvenson, J. Catal. 2 (1963) 58–62.
[10] W.M.H. Sachtler, Recl. Trav. Chim. 82 (1963) 243–245.
[11] L.D. Krenzke, G.W. Keulks, J. Catal. 61 (1980) 316–325.
[12] W. Ueda, K. Asakawa, C.L. Chen, Y. Moro-Oka, T. Ikawa, J. Catal. 101 (1986) 360–368.
[13] G.W. Keulks, J. Catal. 19 (1970) 232–235.
[14] B. Grzybowska, J. Haber, J. Janas, J. Catal. 49 (1977) 150–163.
[15] J. Haber, W. Turek, J. Catal. 190 (2000) 320–326.
[16] W.J. Linn, A.W. Sleight, J. Catal. 41 (1976) 134–139.
[17] I. Matsuura, G.C.A. Schuit, J. Catal. 20 (1971) 19–39.
[18] M. Oliveira, M.F. Portela, M.J. Pires, F.R. Riebeiro, Can. J. Chem. Eng. 61 (1983) 87–92.
[19] J.C. Jung, H. Kim, A.S. Choi, Y.-M. Chung, T.J. Kim, S.J. Lee, S.-H. Oh, I.K. Song, J. Mol. Catal. A 259 (2006) 166–170.
[20] B. Grzybowska, J. Haber, J. Komorek, J. Catal. 25 (1972) 25–32.
[21] E.V. Hoefs, J.R. Monnier, G.W. Keulks, J. Catal. 57 (1979) 331–337.
[22] M.W.J. Wolfs, P.H.A. Bastist, J. Catal. 32 (1974) 25–36.
[23] P. Mars, D.W. van Krevelen, Chem. Eng. Sci. 3 (1954) 41–59.
[24] R.K. Grasselli, Top. Catal. 21 (2001) 79–88.
[25] R.K. Grasselli, J. Chem. Educ. 63 (1986) 216–221.
[26] C.R. Adams, H.H. Voge, C.Z. Zorgan, W.E. Armstrong, J. Catal. 3 (1964) 379–386.
[27] P.H.A. Batist, C.J. Kapteijns, B.C. Lippens, G.C.A. Schuit, J. Catal. 7 (1967) 33–49.
[28] C.R. Adams, T.T.J. Jennings, J. Catal. 2 (1963) 63–68.
[29] A.C.A.M. Bleijenberg, B.C. Lippens, G.C.A. Schuit, J. Catal. 4 (1965) 581–585.
[30] P.H.A. Batist, A.H.W.M. Der Kinderen, Y. Leeuwenburgh, F.A.M.G. Mets, G.C.A. Schuit, J. Catal. 12 (1968) 45–60.
[31] R.S. Mann, D.W. Ko, J. Catal. 30 (1973) 276–282.
[32] F. Benyahia, A.M. Mearns, Appl. Catal. 66 (1990) 383–393.
[33] F. Benyahia, A.M. Mearns, Appl. Catal. 70 (1991) 149–159.
[34] M. Cesari, G. Perego, A. Zazzetta, G. Manara, G. Notari, J. Inorg. Nucl. Chem. 33 (1971) 3595–3597.
[35] A.W. Sleight, K. Aykan, D.B. Rogers, J. Solid State Chem. 13 (1975) 231–236.
[36] A.W. Sleight, W.J. Linn, Ann. N. Y. Acad. Sci. 272 (1976) 22–44.
[37] Z. Zhai, A. Getsoian, A.T. Bell, J. Catal. 308 (2013) 25–36.
[38] A. Getsoian, V. Shapovalov, A.T. Bell, J. Phys. Chem. C 117 (2013) 7123–7137.
[39] A. Getsoian, A.T. Bell, J. Phys. Chem. C 117 (2013) 25562–25578.
[40] R.E. Jentoft, S.E. Deutsch, B.C. Gates, Rev. Sci. Instrum. 67 (1996) 2111–2112.
[41] K. Keizer, PH.A. Batist, G.C. Schuit, J. Catal. 15 (1969) 256–266.
[42] Y. Moro-oka, Catal. Today 45 (1998) 3–12.
[43] M. Krivanek, P. Jiri, J. Strnad, J. Catal. 23 (1971) 259–269.
[44] A. Getsoian, Z. Zhai, A.T. Bell, J. Am. Chem. Soc. 136 (2014) 13684–13697.